Hybrid Force and Position Control Strategy of Robonaut Performing Object Transfer Task

Gang Chen, Yu-Qi Wang , Qing-Xuan Jia and Pei-Lin Cai

School of Automation, Beijing University of Posts and Telecommunications, Beijing 100876, China

Abstract. This paper proposes a coordinated hybrid force/position control strategy of robonaut performing object transfer operation. Firstly, the constraint relationships between robonaut and object are presented. Base on them, the unified dynamic model of the robonaut and object is established to design the hybrid force/position control method. The movement, the internal force and the external constraint force of the object are considered as the control targets of the control system. Finally, a MATLAB simulation of the robonaut performing object transfer task verifies the correctness and effectiveness of the proposed method. The results show that all the targets can be control accurately by using the method proposed in this paper. The presented control method can control both internal and external forces while maintaining control accuracy, which is a common control strategy.

1 Introduction

The complexity and difficulty of space missions increase alongside the deepening of human exploration about space. Therefore, a new type of space robot called robonaut is designed to deal with this situation, and it can be used to assist or replace the human astronauts to carry out the on-orbit operation tasks in order to reduce the astronauts' working pressure and the cost of space operations. The robonaut consist of three branches, in which one is generally called the coupled torso while the other two are robot arms. Due to the existence of redundant arms, its flexibility, operation ability, operating range and other aspects of performance are far better than single arm robot, and its coordination ability and control accuracy are significantly improved compared with the multi robot because of the existence of coupled torso. The robonaut, with its strong collaboration and wide operating range, can efficiently and reliably assist astronauts in performing many on-orbit operations, including mating, twisting, handling, complex parts assembling and space station maintenance etc. As a typical dual arm coordination task, object transfer is representative in orbit operation, so it is of great significance to study the coordinated operation method in the process of object transfer.

The position control strategy is difficult to meet the requirements of the interaction between the robot and the environment when the robonaut performs coordinated manipulation tasks. To finely perform the given task, compliance control method is necessary which means it is vital to control the necessary operation force in the coordinated manipulation tasks, as well as limit the undesirable force to the system meanwhile. There are several main manners of dual-arm coordinate operate control technique, such as impedance control[1-2], hybrid force/position control [3-4], intelligent control[5-6]. The hybrid force/position control method is relatively simple and does not rely on environmental information. Besides, the accuracy of this method is relatively higher than other methods. Given this, the hybrid force/position control method is adopted in this paper.

A number of relevant researches have been carried out which concerning the hybrid force/position control during the processes of object transfer. C. V. Albrichsfeld [7] analyzed the relationship in two robots holding a single object by introducing a concept of 'virtual stick', and then they presented a symmetric non-master/slave hybrid position/force coordinated control scheme using the equations which derive from virtual stick. A. I. Tuneski [8] extended an active compliance control scheme which is capable of adjusting its parameters to the unknown system compliance. Furthermore, a general model was derived by discussing different contact cases of the object. However, all the methods mentioned above existing the following deficiencies: firstly, these articles could not achieve the external force compliance control only considering the internal force when the object is subjected to external force, which may cause the failure of compliance control. Secondly, some of the methods directly divide the object into two parts and then fixed on the end of each manipulator. In this way, a rather better simulation results can be obtained, but these methods are limited to theoretical analysis and are not suitable for practical operation.

For the deficiencies above, more specific study will be carried out in subsequent chapters. Specifically, in chapter II, the constraint relationships between robonaut

and object will be presented. Then, in chapter III, the unified dynamic model of the robonaut and object is going to be established to design the hybrid force/position control method. Moreover, a simulation study will be implemented to verify the algorithm control in chapter IV. Finally, the comprehensive review and summary will be done in the final chapter.

2 Dynamic modeling

The structure of robonaut studied in this paper is shown in Figure 1. It consists of three branches: the coupled torso branch (branch 1) and two arm branches (branch 2 and branch 3). Generally, one end of the coupled torso branch is fixed at the base, the other end is connected with the root of the two arm branches. The ends of the arms are free to move to complete the operational tasks. Assume that branch 1 has $n_1-\text{DOF}$, branch 2 and branch 3 have $n_2-\text{DOF}$ and $n_3-\text{DOF}$ respectively.

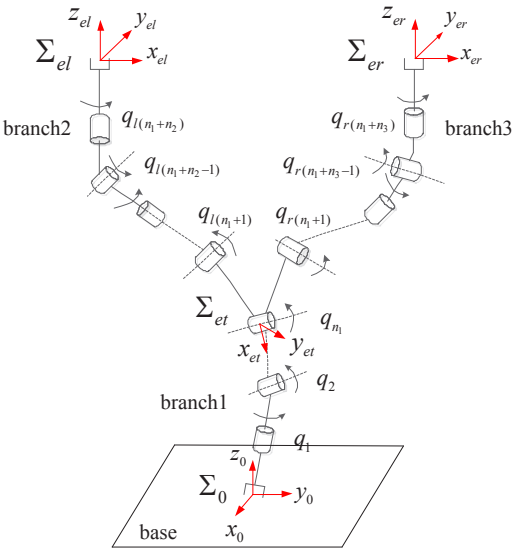

Figure 1. The structure of robonaut

2.1 Constraint relationships

Figure 2 shows the coordinated model of object transfer operation. Point O_c is the mass of the object and the object frame is attached at it. For simplicity, let us ignore the size of object, and translate the origins of the left and right arms end frames to the point O_c, named as $O_{ew}(w=l,r)$.

When we assume that the stiffness of the object is large enough to ignore the deformation, the pose constraint between robonaut and object can be written as

$$\begin{cases} \boldsymbol{P}_c = \boldsymbol{P}_l = \boldsymbol{P}_r \\ {}^0\boldsymbol{R}_c = {}^0\boldsymbol{R}_l\,{}^l\boldsymbol{R}_c = {}^0\boldsymbol{R}_r\,{}^r\boldsymbol{R}_c \end{cases} \tag{1}$$

The velocity constraint can be written as

$$\dot{\boldsymbol{X}}_c = \dot{\boldsymbol{X}}_l = \dot{\boldsymbol{X}}_r \tag{2}$$

The acceleration constraint can be written as

$$\ddot{\boldsymbol{X}}_c = \ddot{\boldsymbol{X}}_l = \ddot{\boldsymbol{X}}_r \tag{3}$$

The force constraint relationship is shown in Figure 3. The output forces of left and right arms, the external constraint force of robonaut system are $\boldsymbol{F}_w = \begin{bmatrix} \boldsymbol{f}_w^{\mathrm{T}} & \boldsymbol{n}_w^{\mathrm{T}} \end{bmatrix}^{\mathrm{T}} (w=l,r,f)$, and translate them to the point O_c, named as $\boldsymbol{F}_{cw} = \begin{bmatrix} \boldsymbol{f}_{cw}^{\mathrm{T}} & \boldsymbol{n}_{cw}^{\mathrm{T}} \end{bmatrix}^{\mathrm{T}} (w=l,r,f)$.

The resultant force of the object can be expressed as

$$\boldsymbol{F}_c = \boldsymbol{W}\boldsymbol{F}_e + \boldsymbol{F}_{cf} \tag{4}$$

where $\boldsymbol{W} = [\boldsymbol{E}_6 \quad \boldsymbol{E}_6]$, $\boldsymbol{F}_e = [\boldsymbol{F}_{cl}^{\mathrm{T}}, \ \boldsymbol{F}_{cr}^{\mathrm{T}}]^{\mathrm{T}}$.

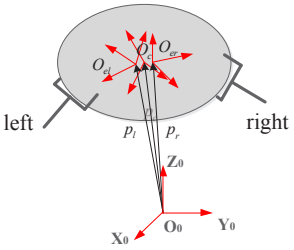

Figure 2. The coordinated model of object transfer operation.

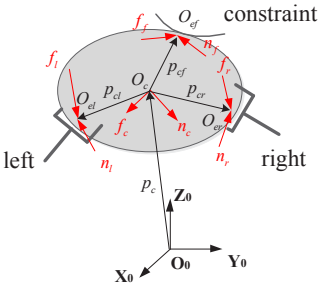

Figure 3. The force model of object transfer operation.

2.2 Dynamic models

In this paper, we intend to use the movement, the internal force and the external constraint force of the object as the control targets of the control system. Firstly, the dynamic models of the object and the robonaut are established. Base on them, the unified dynamic model is constructed, which means the object and the robonaut as a whole.

2.2.1 Object dynamic model

The dynamic equation of object is given by using the Newton-Euler equation

$$\begin{cases} m_c\dot{\boldsymbol{v}}_c = \boldsymbol{f}_c \\ \boldsymbol{I}_c\dot{\boldsymbol{\omega}}_c + \boldsymbol{\omega}_c \times (\boldsymbol{I}_c\boldsymbol{\omega}_c) = \boldsymbol{n}_c \end{cases} \tag{5}$$

where m_c, $\boldsymbol{I}_c$ represent the object's mass and inertia tensor, respectively.

Equation (5) can be rewritten as

$$\boldsymbol{F}_c = \boldsymbol{M}_c\ddot{\boldsymbol{X}}_c + \boldsymbol{C}_c \tag{6}$$

where $\boldsymbol{M}_c = \begin{bmatrix} m_c\boldsymbol{E}_3 & \boldsymbol{0}_{3\times3} \\ \boldsymbol{0}_{3\times3} & \boldsymbol{I}_c \end{bmatrix}$, $\boldsymbol{C}_c = \begin{bmatrix} \boldsymbol{0}_{3\times1} \\ \boldsymbol{\omega}_c \times (\boldsymbol{I}_c\boldsymbol{\omega}_c) \end{bmatrix}$.

2.2.2 Robonaut dynamic model

The velocity of the ends of the arms can be written as $\dot{\boldsymbol{X}}_w = \left[\boldsymbol{v}_w^{\mathrm{T}}, \boldsymbol{\omega}_w^{\mathrm{T}}\right]^{\mathrm{T}} \left(w = l, r\right)$, where $\boldsymbol{v}_w$ and $\boldsymbol{\omega}_w$ are the linear and angular velocity respectively. By differential kinematics, it can be obtained that

$$\begin{cases} \dot{\boldsymbol{X}}_l = [\boldsymbol{v}_l^{\mathrm{T}}, \boldsymbol{\omega}_l^{\mathrm{T}}]^{\mathrm{T}} = \boldsymbol{J}_l \dot{\boldsymbol{q}}_l = \left[\boldsymbol{J}_{l1}, \boldsymbol{J}_{l2}\right] \dot{\boldsymbol{q}}_l \\ \dot{\boldsymbol{X}}_r = [\boldsymbol{v}_r^{\mathrm{T}}, \boldsymbol{\omega}_r^{\mathrm{T}}]^{\mathrm{T}} = \boldsymbol{J}_r \dot{\boldsymbol{q}}_r = \left[\boldsymbol{J}_{r1}, \boldsymbol{J}_{r3}\right] \dot{\boldsymbol{q}}_r \end{cases} \tag{7}$$

where $\boldsymbol{J}_w \left(w = l, r\right)$ represent the Jacobian matrixes of the left and right manipulators respectively.

According to equation (7), the kinematics equation can be thus written as

$$\dot{\boldsymbol{X}}_e = \begin{bmatrix} \dot{\boldsymbol{X}}_l \\ \dot{\boldsymbol{X}}_r \end{bmatrix} = \begin{bmatrix} \boldsymbol{J}_{l1} & \boldsymbol{J}_{l2} & \boldsymbol{0}_{6\times n_3} \\ \boldsymbol{J}_{r1} & \boldsymbol{0}_{6\times n_2} & \boldsymbol{J}_{r3} \end{bmatrix} \dot{\boldsymbol{q}} = \boldsymbol{J}\dot{\boldsymbol{q}} \tag{8}$$

where $\boldsymbol{J} \in \mathbf{R}^{12\times(n_1+n_2+n_3)}$ represents the Jacobian matrix of the robonaut.

From equation (8), we can get

$$\begin{cases} \ddot{\boldsymbol{X}}_e = \dot{\boldsymbol{J}}\dot{\boldsymbol{q}} + \boldsymbol{J}\ddot{\boldsymbol{q}} \\ \ddot{\boldsymbol{q}} = \boldsymbol{J}^{+}\left(\ddot{\boldsymbol{X}}_e - \dot{\boldsymbol{J}}\dot{\boldsymbol{q}}\right) \end{cases} \tag{9}$$

where $\boldsymbol{J}^{+}$ represents pseudo-inverse of $\boldsymbol{J}$.

By using Lagrange-Euler method, the dynamics of the robonaut in joint space coordinates suggested in this paper can be described as follows

$$\boldsymbol{A}(\boldsymbol{q})\ddot{\boldsymbol{q}} + 2\boldsymbol{B}(\boldsymbol{q})\dot{\boldsymbol{q}}_m\dot{\boldsymbol{q}}_n + \boldsymbol{C}(\boldsymbol{q})\dot{\boldsymbol{q}}^2 + \boldsymbol{D}(\boldsymbol{q}) + \boldsymbol{J}^{\mathrm{T}}\boldsymbol{F}_e = \boldsymbol{\tau} \tag{10}$$

where $\boldsymbol{A}(\boldsymbol{q})$ is an $n\times n$ symmetric positive definite inertia matrix. $\boldsymbol{A}(\boldsymbol{q})\ddot{\boldsymbol{q}}$ represents the inertia forces vector. $\boldsymbol{B}(\boldsymbol{q})$ is an $n\times\left[n(n-1)/2\right]$ Coriolis matrix. $2\boldsymbol{B}(\boldsymbol{q})\dot{\boldsymbol{q}}_m\dot{\boldsymbol{q}}_n$ represents the Coriolis forces vector. $\boldsymbol{C}(\boldsymbol{q})$ is an $n\times n$ centrifugal matrix. $\boldsymbol{C}(\boldsymbol{q})\dot{\boldsymbol{q}}^2$ represents the centrifugal forces vector. $\boldsymbol{D}(\boldsymbol{q})$ is an $n\times 1$ gravitational matrix. In addition, $n = n_1 + n_2 + n_3$.

Substituting (9) to(10), the dynamics of the robonaut in Cartesian space coordinates can be described as

$$\boldsymbol{M}\ddot{\boldsymbol{X}}_e + \boldsymbol{C} + \boldsymbol{F}_e = \boldsymbol{U} \tag{11}$$

Where

$$\begin{cases} \boldsymbol{M} = \boldsymbol{J}^{+\mathrm{T}}\boldsymbol{A}(\boldsymbol{q})\boldsymbol{J}^{+} \\ \boldsymbol{C} = \boldsymbol{J}^{+\mathrm{T}}\left[2\boldsymbol{B}(\boldsymbol{q})\dot{\boldsymbol{q}}_m\dot{\boldsymbol{q}}_n + \boldsymbol{C}(\boldsymbol{q})\dot{\boldsymbol{q}}^2 + \boldsymbol{D}(\boldsymbol{q})\right] - \boldsymbol{M}\dot{\boldsymbol{J}}\dot{\boldsymbol{q}} \\ \boldsymbol{U} = \boldsymbol{J}^{+\mathrm{T}}\boldsymbol{\tau} \end{cases}$$

2.2.3 Robonaut system unified dynamic model

From(4), the output force of robonaut can be obtained as

$$\begin{aligned} \boldsymbol{F}_e &= \boldsymbol{W}^{+}\left(\boldsymbol{F}_c - \boldsymbol{F}_{cf}\right) + \left(\boldsymbol{E}_{12} - \boldsymbol{W}^{+}\boldsymbol{W}\right)\begin{bmatrix}\boldsymbol{\eta}_l \\ \boldsymbol{\eta}_r\end{bmatrix} \\ &= \boldsymbol{W}^{+}\left(\boldsymbol{M}_c\ddot{\boldsymbol{X}}_c + \boldsymbol{C}_c\right) - \boldsymbol{W}^{+}\boldsymbol{F}_{cf} + \boldsymbol{W}_i\boldsymbol{F}_i \end{aligned} \tag{12}$$

① The first term on the right side of the equation, represents the driving force of robonaut on the object, where $\boldsymbol{W}^{+} = [\boldsymbol{E}_6,\ \boldsymbol{E}_6]^{\mathrm{T}}/2$.

② The second term on the right side of the equation, represents the external constraint force of robonaut system.

③ The third term on the right side of the equation, $\left(\boldsymbol{E}_{12} - \boldsymbol{W}^{+}\boldsymbol{W}\right)$ represents the null space of $\boldsymbol{W}$, $\boldsymbol{\eta}_w \left(w = l, r\right)$ represents any 6×1 vector. Due to the characteristics of null space, we can get that $\boldsymbol{W}\left(\boldsymbol{E}_{12} - \boldsymbol{W}^{+}\boldsymbol{W}\right)\left[\boldsymbol{\eta}_l^{\mathrm{T}},\ \boldsymbol{\eta}_r^{\mathrm{T}}\right]^{\mathrm{T}} = \boldsymbol{0}_{6\times 1}$. So, this part of force produces the internal force of the object. Also, $\boldsymbol{W}_i = \left[\boldsymbol{E}_6,\ -\boldsymbol{E}_6\right]^{\mathrm{T}}$, $\boldsymbol{F}_i = \left(\boldsymbol{\eta}_l - \boldsymbol{\eta}_r\right)/2$.

Substituting (3), (12) to (11), the unified dynamic model is constructed as

$$\boldsymbol{U} = \boldsymbol{M}_s\ddot{\boldsymbol{X}}_c + \boldsymbol{C}_s - \boldsymbol{W}^{+}\boldsymbol{F}_{cf} + \boldsymbol{W}_i\boldsymbol{F}_i \tag{13}$$

where：

$$\begin{cases} \boldsymbol{M}_s = \boldsymbol{M} + \boldsymbol{W}^{+}\boldsymbol{M}_c \\ \boldsymbol{C}_s = \boldsymbol{C} + \boldsymbol{W}^{+}\boldsymbol{C}_c \end{cases} \tag{14}$$

3 Control algorithm

In this paper, the internal force, the movement and the external constraint force of the object are considered as the control targets of the hybrid force/position control system. To simplify the problem, the internal force at the mass center of the object can be chosen in object transfer operation task.

The position control law of object can be designed as

$$\ddot{\boldsymbol{X}}_c = \bar{\boldsymbol{S}}\left[\ddot{\boldsymbol{X}}_{cd} + \boldsymbol{K}_d\left(\dot{\boldsymbol{X}}_{cd} - \dot{\boldsymbol{X}}_c\right) + \boldsymbol{K}_p\left(\boldsymbol{X}_{cd} - \boldsymbol{X}_c\right)\right] \tag{15}$$

where $\boldsymbol{X}_{cd}$, $\dot{\boldsymbol{X}}_{cd}$ and $\ddot{\boldsymbol{X}}_{cd}$ represent the desired pose, velocity and acceleration respectively. $\boldsymbol{K}_p$, $\boldsymbol{K}_d$ are derivative and proportional feedback gains respectively. $\bar{\boldsymbol{S}}$ is an 6×6 position-selecting matrix.

The external constraint force control law of the robonaut system can be designed as

$$\boldsymbol{F}_{cf} = \boldsymbol{S}\left[\boldsymbol{F}_{cfd} + \boldsymbol{K}_{pf}\left(\boldsymbol{F}_{cfd} - \boldsymbol{F}_{cf}\right) + \boldsymbol{K}_{df}\left(\dot{\boldsymbol{F}}_{cfd} - \dot{\boldsymbol{F}}_{cf}\right)\right] \tag{16}$$

where $\boldsymbol{F}_{cfd}$ represent the desired external constraint force. $\boldsymbol{K}_{pf}$, $\boldsymbol{K}_{df}$ are derivative and proportional feedback gains respectively. $\boldsymbol{S}$ is an 6×6 force-selecting matrix.

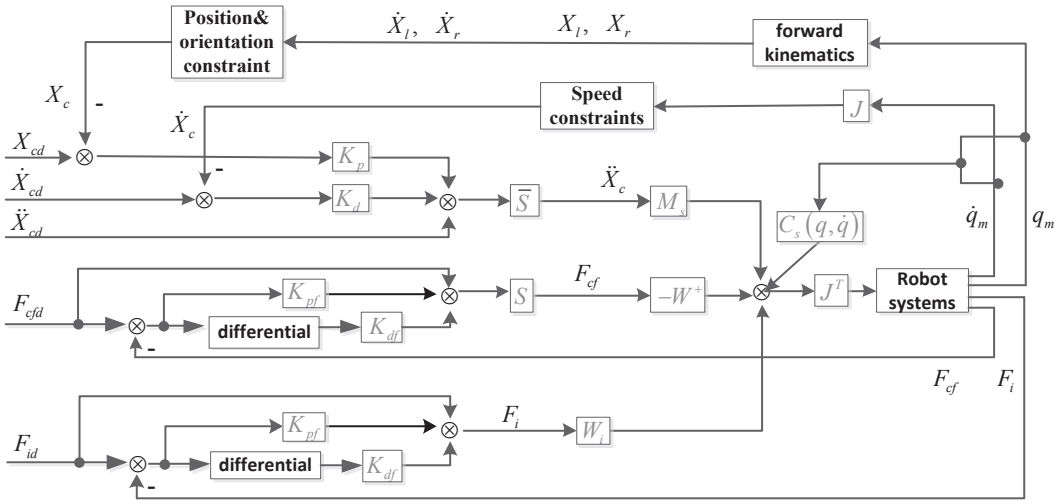

Figure 4. Hybrid force/position control structure of robonaut.

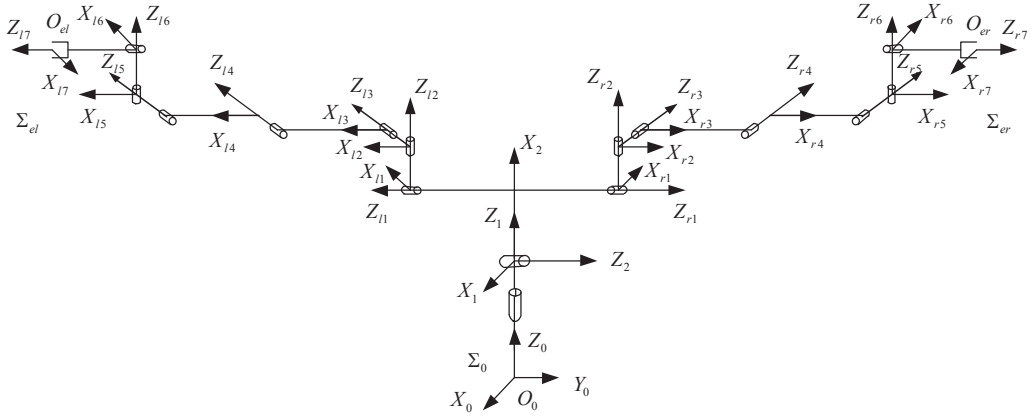

Figure 5. D-H frames of robonaut in simulation.

The internal force control law of the object can be designed as

$$\boldsymbol{F}_{ic} = \boldsymbol{F}_{id} + \boldsymbol{K}_{pi}\left(\boldsymbol{F}_{id} - \boldsymbol{F}_{i}\right) + \boldsymbol{K}_{di}\left(\dot{\boldsymbol{F}}_{id} - \dot{\boldsymbol{F}}_{i}\right) \tag{17}$$

where $\boldsymbol{F}_{id}$ represent the desired internal force.

Substituting(15), (16) (17) to (13) it can be obtained that the control joint torque

$$\begin{aligned}\boldsymbol{\tau} = \boldsymbol{J}^{\mathrm{T}}\Big[&\boldsymbol{M}_s\bar{\boldsymbol{S}}\left(\ddot{\boldsymbol{X}}_{cd} + \boldsymbol{K}_d\left(\dot{\boldsymbol{X}}_{cd} - \dot{\boldsymbol{X}}_c\right) + \boldsymbol{K}_p\left(\boldsymbol{X}_{cd} - \boldsymbol{X}_c\right)\right)\\ &+\boldsymbol{C}_s - \boldsymbol{W}^{+}\boldsymbol{S}\left(\boldsymbol{F}_{cfd} + \boldsymbol{K}_{pf}\left(\boldsymbol{F}_{cfd} - \boldsymbol{F}_{cf}\right) + \boldsymbol{K}_{df}\left(\dot{\boldsymbol{F}}_{cfd} - \dot{\boldsymbol{F}}_{cf}\right)\right)\\ &+\boldsymbol{W}_i\left(\boldsymbol{F}_{id} + \boldsymbol{K}_{pi}\left(\boldsymbol{F}_{id} - \boldsymbol{F}_{i}\right) + \boldsymbol{K}_{di}\left(\dot{\boldsymbol{F}}_{id} - \dot{\boldsymbol{F}}_{i}\right)\right)\Big]\end{aligned} \tag{18}$$

The proposed control structure is shown in Figure 4.

4 Simulation Study

The robonaut involved in this simulation is shown in Figure 5. The coupled torso has 2 rotation joints and the two arms both have 7 rotation joints. The D-H parameters of the robonaut are listed in Table 1.

Table 1. D-H parameters of the robonaut in simulation.

	α_{i-1} / rad	a_{i-1} / m	θ_i / rad	d_i / m
t1	0	0	0	0.45
t2	-π/2	0	-π/2	0
al1	π	0.3	-π	0.2
al2	π/2	0	π/2	0.15
al3	π/2	0	0	0.15
al4	0	0.5	0	0.15
al5	0	0.5	0	0.15
al6	-π/2	0	-π/2	0.15
al7	-π/2	0	-π	0.2
ar1	0	0.3	π	0.2
ar2	-π/2	0	-π/2	0.15
ar3	-π/2	0	0	0.15
ar4	0	0.5	0	0.15
ar5	0	0.5	0	0.15
ar6	π/2	0	π/2	0.15
ar7	π/2	0	π	0.2

The task involved in this simulation is that the robonaut holds an object to terminal point along a desired arc trajectory on the constraint surface. Assuming that the radius of the arc is 0.1m, and the object must remain in contact with the constraint surface during the movement. Set the total control time to be 10s.

Assuming that the constraint surface is parallel to the inertial frame yOz plane. The origin of the constraint frame is set at the center of the arc trajectory. Then the homogeneous transformation matrixes representing the poses of constraint frame with respect to inertial frame is $\boldsymbol{R}_{0c}$ =[0, 0, -1; 1, 0, 0; 0, -1, 0].

The initial position of object is $\boldsymbol{P}_{c\_int}$=[-0.5m, 0.1m, 1.5m], the corresponding joint angle is $\boldsymbol{q}_{l0}$ =[-1.34° , -15.88°], $\boldsymbol{q}_{l0}$ =[47.09° , -131.02° , 186.84° , -94.48° , 157.38° , 161.55° , 38.06°], $\boldsymbol{q}_{r0}$ =[-53.89° , 142.63° , -194.46° , 90.40° , -152.17° , -164.75° , -50.64°]. The desired internal force is set as $\mathbf{0}_{6\times1}$, the desired external constraint force is set as $\mathbf{0}_{6\times1}$.

Apply the algorithm mentioned above to this case, then the trajectory , the internal force and the external constraint force of the object result to be Figure 6, Figure 7 and Figure 8 respectively, which verifies the effectiveness of the algorithm discussed in this paper.

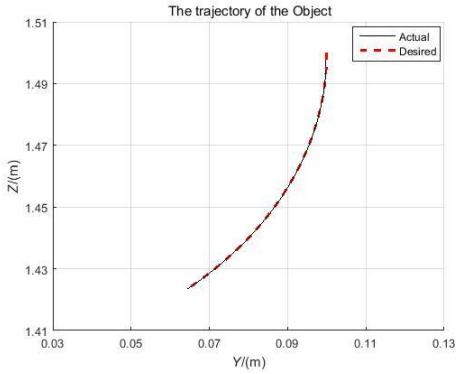

Figure 6. The trajectory of the object.

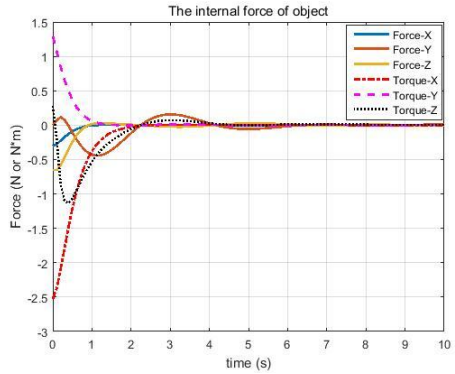

Figure 7. The internal force of the object.

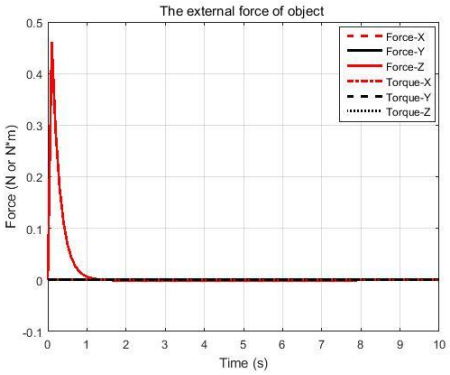

Figure 8. The external force of the object.

5 Conclusion

This paper proposes the coordinated hybrid force/position control strategy of robonaut performing object transfer operation. The constraint relationship between two manipulators and object is presented at first. Afterward the unified dynamic model of the robonaut and object is established to design the hybrid force/position control method of the robonaut. The movement, the internal force and the external constraint force of the object are considered as the control targets of the control system, thereby achieving simultaneous control of the internal force and the external force of the object. Finally a simulation study verifies the effectiveness of the algorithm.

References

1. Y L. Kim, B S. Kim, J B Song. *IEEE CASE*., 1074(2012)
2. J. Lu, J P. Yan, J J. Chen. Con Theo & Appl. **20**(1), 85(2003).
3. W F. Xu, R X. Zhou, D S. Meng. Journal of Astronautics, **34**(10), 1353(2013).
4. K. Zhang, Q. Wei, W S.Chang. ROBOT, **24**(1), 44(2002).
5. S T. Lin, A K. Huang. J Intell Rob Syst Theor Appl, **19**(4), 393(1997).
6. A. A. G. Siqueira, M. H. Terra. *ACC*, **17**(3), 418(2009).
7. C V. Albrichsfeld, H. Tolle. Control Eng. Pract., **10**(2), 165(2002).
8. A I. Tuneski, M K. Vukobratovic, G M. Dim. Acou Spe & Sig Proce News. **215**(4), 385(2001).